Applied and Computational Harmonic Analysis **10**, 163–181 (2001)
doi:10.1006/acha.2000.0332, available online at http://www.idealibrary.com on IDEAL®

LETTER TO THE EDITOR

Smooth Wavelet Tight Frames with Zero Moments

Ivan W. Selesnick [1]

Department of Electrical Engineering, Polytechnic University, 6 Metrotech Center, Brooklyn, New York 11201
E-mail: selesi@taco.poly.edu

Communicated by Charles K. Chui
Received June 7, 2000; revised October 5, 2000

Abstract—This paper considers the design of wavelet tight frames based on iterated oversampled filter banks. The greater design freedom available makes possible the construction of wavelets with a high degree of smoothness, in comparison with orthonormal wavelet bases. In particular, this paper takes up the design of systems that are analogous to Daubechies orthonormal wavelets—that is, the design of minimal length wavelet filters satisfying certain polynomial properties, but now in the oversampled case. Gröbner bases are used to obtain the solutions to the nonlinear design equations. Following the dual-tree DWT of Kingsbury, one goal is to achieve near shift invariance while keeping the redundancy factor bounded by 2, instead of allowing it to grow as it does for the undecimated DWT (which is exactly shift invariant). Like the dual tree, the overcomplete DWT described in this paper is less shift-sensitive than an orthonormal wavelet basis. Like the examples of Chui and He, and Ron and Shen, the wavelets are much smoother than what is possible in the orthonormal case.

Key Words: overcomplete signal expansions; wavelets; frames.

1. INTRODUCTION

Frames, or overcomplete expansions, have a variety of attractive features. With frames, better time-frequency localization can be achieved than is possible with bases. Some wavelet frames can be shift invariant, while wavelet bases cannot be. Frames provide more degrees of freedom to carry out design. Several applications have benefited from the use of frames, for example, denoising [3, 9, 23, 39] and signal coding [15, 25]. There are a number of methods of generating practical frames.

1. The *undecimated DWT* (UDWT) generates a wavelet frame from an existing wavelet basis by removing the subsampling from an existing critically sampled filter bank, see [9, 18, 26, 29, 36].

2. A wavelet frame can be obtained by taking the union of two (or more) bases. This can be implemented with two independent filter banks operating in parallel. Kingsbury has shown the advantages of *dual-tree DWTs* in [19, 20].

[1] Research supported by NSF under CAREER Grant CCR-987452.

1063-5203/01 $35.00

3. A wavelet frame can also be obtained by iterating a suitably designed oversampled filter bank as developed in [7, 30, 31], for example. This is the type of frame to be considered in this paper.

Of these three methods, only the undecimated DWT generates a truly time-invariant discrete transform. However, the UDWT has an expansion factor of $\log N$: it expands an N-sample data vector to $N \log N$ samples. For very large data sets, like images, this data expansion can make it difficult to use in practice. On the other hand, the dual-tree DWT, and the oversampled DWT to be described below, expands an N-sample data vector to $2N$ samples—independent of the number of scales over which the signal decomposition is performed. While it does not yield exactly shift-invariant discrete transforms, Kingsbury has shown that, nevertheless, the dual-tree DWT can be made very nearly time invariant by suitably designing two filter banks to work together. [2]

This paper describes new wavelet tight frames based on iterated oversampled FIR filter banks, first introduced in [35]. The setting is the same as [7, 30]; however, the design problem under consideration and the approach are different. In particular, this paper takes up the design of systems that are analogous to Daubechies orthonormal wavelets [12]—that is, the design of minimal length wavelet filters satisfying certain polynomial properties, but now in the oversampled case. It should be noted that in the oversampled case, if a wavelet is very smooth it does not mean that its moments $\int t^k \psi(t)\, dt$ are zero (or small) for $k > 0$, in sharp contrast to the orthonormal case. The smoothness and zero moments properties are less related than in the critically sampled case. Like the examples by Chui and He [7] and Ron and Shen [30], the wavelets presented below are much smoother than what can be achieved in the critically sampled case; however, in this paper the zero moments properties of the wavelets are also taken into account. For a given number of wavelet moments and a given number of zeros at $z = -1$ of the scaling filter $H_0(z)$, the wavelets presented below are of minimal length.

In [7, 30] methods are given to generate a tight wavelet frame corresponding to a specified refinable function (scaling function). The approach taken in this paper is to treat the scaling and wavelet functions together as unknown. The nonlinear design equations that arise are then solved using Gröbner bases. As Gröbner bases are used in this paper to carry out the design, we are able to obtain zero wavelet moments for wavelets of minimal length, in contrast to earlier work on wavelet tight frames of this type. Although the high computational and memory cost of Gröbner bases limits their utility, we are able to obtain solutions of practical interest. In addition, software for Gröbner bases is improving with time.

In addition, like Kingsbury's dual-tree DWT, the frames presented in this paper are less shift-sensitive than orthonormal wavelet bases, even though the redundancy rate is only 2, independent of the number of scales over which the signal expansion is performed. Because the frames described in this paper are based on iterated FIR filter banks, a fast discrete frame transform is simple to implement. This paper considers exclusively *tight* frames.

[2] Kingsbury's dual-tree DWT is designed to act as a complex wavelet transform; however, that interpretation does not apply to the frames to be presented here.

2. WAVELET TIGHT FRAMES AND ITERATED OVERSAMPLED FILTER BANKS

2.1. Preliminaries

For in-depth analysis of oversampled filter banks and frames, see for example [1, 4, 8, 11, 12, 30, 31]. Here the notation and basic framework is given. We follow a framework that closely resembles the standard multiresolution framework leading to orthonormal dyadic wavelet bases. Each of the wavelet tight frames to be developed in this paper will be based on a single-scaling function $\phi(t)$ and two distinct wavelets $\psi_1(t)$ and $\psi_2(t)$. (We label the wavelets as ψ_1, ψ_2 instead of ψ_0, ψ_1 as it will simplify notation.) Following the theory of dyadic wavelet bases, the scaling space $\mathcal{V}_j$ and the wavelet spaces $\mathcal{W}_{i,j}$ are defined as

$$\mathcal{V}_j = \operatorname*{Span}_{n\in\mathbb{Z}}\{\phi(2^j t - n)\}$$
$$\mathcal{W}_{i,j} = \operatorname*{Span}_{n\in\mathbb{Z}}\{\psi_i(2^j t - n)\}, \qquad i = 1, 2.$$

(Of course, dyadic wavelet *bases* are based on a single-scaling function ϕ and a single wavelet ψ. The extra wavelet here makes this system an overcomplete one.) Following the multiresolution framework, one asks that these signal spaces be nested: $\mathcal{V}_0 \subset \mathcal{V}_1$, $\mathcal{W}_{1,0} \subset \mathcal{V}_1$, $\mathcal{W}_{2,0} \subset \mathcal{V}_1$. It follows that ϕ, ψ_1, ψ_2 satisfy the dilation and wavelet equations

$$\phi(t) = \sqrt{2}\sum_n h_0(n)\phi(2t - n)$$
$$\psi_i(t) = \sqrt{2}\sum_n h_i(n)\phi(2t - n), \qquad i = 1, 2.$$

Corresponding to ϕ, ψ_1, ψ_2, we have the scaling filter $h_0(n)$, the two wavelet filters $h_1(n)$ and $h_2(n)$, and the oversampled filter bank illustrated in Fig. 1. The transfer function $H_i(z)$ is given by $\sum_n h_i(n)z^{-n}$. Note that throughout the paper, $t \in \mathbb{R}$, $i, j, k, l, m, n \in \mathbb{Z}$.

Let $\phi_k(t) = \phi(t - k)$ and $\psi_{i,j,k}(t) = \psi_i(2^j t - k)$ for $i = 1, 2$. In this paper we consider ϕ, ψ_i for which any square integrable signal $f(t)$ is given by

$$f(t) = \sum_{k=-\infty}^{\infty} c(k)\phi_k(t) + \sum_{j=0}^{\infty}\sum_{k=-\infty}^{\infty} d_1(j,k)\psi_{1,j,k}(t) + d_2(j,k)\psi_{2,j,k}(t), \tag{1}$$

where

$$c(k) = \int f(t)\phi_k(t)\,dt, \qquad d_i(j,k) = \int f(t)\psi_{i,j,k}(t)\,dt, \qquad i = 1, 2.$$

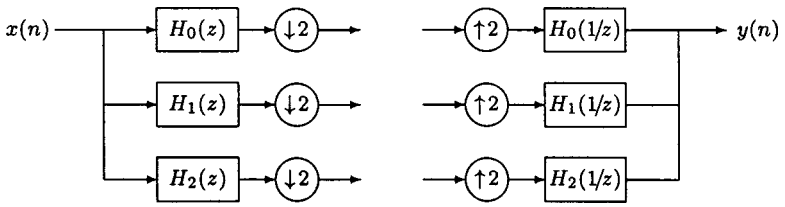

FIG. 1. An oversampled analysis and synthesis filter bank.

That is, the functions $\{\phi_k(t), \psi_{i,j,k}(t) : j, k \in \mathbb{Z},\ j \geq 0,\ i \in \{0, 1\}\}$ form a tight frame for $L_2(\mathbb{R})$. Note that an orthonormal dyadic wavelet basis can be written in this form—with $\psi_2(t) = 0$ and $h_2(n) = 0$ one retrieves the multiresolution framework that leads to orthonormal bases.

From (1), it can be shown that both frame bounds A and B are equal to 1. It should be emphasized that even though $A = B = 1$, the frames to be considered in the paper are not an orthonormal basis because the functions ϕ, ψ_1 and ψ_2 do not have norm 1. $A = B = 1$ means the frame is an orthonormal basis only when $\|\psi_1\| = \|\psi_2\| = 1$, which will not be the case for the tight frames to be described in this paper.

The frame conditions require that $\int \psi_i(t)\, dt = 0$. Therefore, setting $f(t) = 1$ in (1) we get $1 = \sum_k (\int \phi_k(\tau)\, d\tau)\phi_k(t)$ (ignoring that $f(t) = 1$ is not square integrable), or $1 = (\int \phi(t)\, dt)(\sum_k \phi_k(t))$. Using the identity $\sum_k \phi_k(t) = \int \phi(t)\, dt$ (provided ϕ is continuous), one gets $1 = (\int \phi(t)\, dt)^2$. We will use the normalization $1 = \int \phi(t)\, dt$.

2.2. Zeros at $\omega = 0$, $\omega = \pi$

The degrees of freedom in the design of oversampled filter banks can be used in a variety of ways. We emphasize that, in contrast to critically sampled filter banks, there are some important differences with respect to zero wavelet moments and the smoothness properties. It is noted that this can be used to improve the smoothness of the wavelets as in [7, 30]. Let K_0 denote the number of zeros $H_0(e^{j\omega})$ has at $\omega = \pi$. For $i = 1, 2$, let K_i denote the number of zeros $H_i(e^{j\omega})$ has at $\omega = 0$:

$$H_0(z) = Q_0(z)(z + 1)^{K_0}, \qquad H_1(z) = Q_1(z)(z - 1)^{K_1}, \qquad H_2(z) = Q_2(z)(z - 1)^{K_2}.$$

For orthonormal bases ($\psi_2(t) = 0$), it is necessary that $K_0 = K_1$, so no distinction need be made between K_0 and K_1. However, for tight wavelet frames of the form (1), it is not necessary that $K_0 = K_1 = K_2$. K_0 denotes the degree of polynomials representable by shifts of $\phi(t)$ and is related to the smoothness of $\phi(t)$. K_1 and K_2 denote the number of zero moments of the wavelet filters $h_1(n)$ and $h_2(n)$, provided $K_0 \geq K_1$, and $K_0 \geq K_2$. That is, as long as $K_0 \geq K_1$ and $K_0 \geq K_2$, one has

$$\mathcal{P}_{K_0 - 1} \subset \mathcal{V}_0 \qquad \text{and} \qquad \int t^k \psi_i(t)\, dt = 0 \qquad \text{for } k = 0, \ldots, K_i - 1,\ i = 1, 2,$$

resembling the case for orthonormal wavelet bases. ($\mathcal{P}_k$ denotes the space of polynomials of degree k and less.)

The value of K_0 influences the degree of smoothness of ϕ (and therefore of ψ_i). On the other hand, the values K_1 and K_2 indicate what polynomials are annihilated (compressed) by the given signal expansion. In contrast to orthonormal wavelet bases, with a tight frame one has the possibility of controling these parameters more freely. If it is desired for a given class of signals that the wavelets have two zero moments (for example), then the remaining degrees of freedom can be used to achieve a higher degree of smoothness by making K_0 greater than K_1 and K_2.

Although the values K_i need not all be equal, there is still the constraint

$$\text{length } h_0 \geq K_0 + \min(K_1, K_2).$$

This is obtained from

$$|H_0(e^{J\omega})|^2 + |H_1(e^{J\omega})|^2 + |H_2(e^{J\omega})|^2 = 2, \tag{2}$$

which is a consequence of the tight frame conditions (3). So the minimum length of h_0 is $K_0 + \min(K_1, K_2)$. In the orthonormal case $K_0 = K_1$ and $K_2 = \infty$ (as $h_2 = 0$), which gives the minimum length of h_0 to be $2K_0$, which is consistent with Daubechies' orthonormal filters.

2.3. Spline-Based Tight Frames

Ron and Shen present a very interesting example in [30, 31] of a family of wavelet tight frames based on spline functions. In that example, there are K_0 wavelets, and the scaling function ϕ is a spline obtained by convolving the square pulse $p(t)$ with itself K_0 times: $\phi(t) = p(t) * \cdots * p(t)$ (a B spline). K_0 can be any integer, so ϕ can be extremely smooth and symmetric, and approaches the Gaussian as K_0 is increased. In addition, all the wavelets are also symmetric or anti-symmetric. The filters h_i are given by

$$H_i(z) = \sqrt{2}\sqrt{\binom{K_0}{i}}\left(\frac{1+z^{-1}}{2}\right)^{K_0-i}\left(\frac{1-z^{-1}}{2}\right)^{i}$$

for $i = 0, \ldots, K_0$. In this construction the number of wavelets increases with the increase of the smoothness, and the ith wavelet has i zeros at $z = 1$. That is, increasing K_0 increases the redundancy and does not raise the minimum K_i. In particular, ψ_1 has $K_1 = 1$ only.

More recently, Chui and He [7] also introduced wavelet tight frames for the same $\phi(t)$, but with only two wavelets (three if they are to be symmetric and anti-symmetric). This reduces the redundancy; however, in this case at least one of the wavelets does not have more than a single zero moment. Also introduced in [7] are wavelet tight frames based on symmetric interpolating scaling functions, for which $K_0 = K_1 = 2K_2$.

In Section 3, examples of minimal length are given for which the redundancy is limited to 2, and for which $K_1 = K_2 > 1$. However, the filters h_i are not given by a simple formula.

2.4. Norms

It should be emphasized that for a tight frame of this kind, it is not necessary that ψ_1 and ψ_2 have the same norms (L_2 norms). While many examples of tight frames given in the literature are based on functions having equal norms, that is not a requirement in general. In particular, for the examples presented below, we have $\|\psi_1\| \neq \|\psi_2\|$. It is important to know the value of the norms $\|\psi_i\|$ in applications where the wavelet coefficients $\langle f, \psi_i \rangle$ are processed, for example, by quantization in compression, or thresholding in denoising. The quantization and threshold levels must be adjusted according to the norm of ψ_i.

Because closed form expressions for $\phi(t)$ and $\psi_i(t)$ are not available in general, their norms cannot be calculated directly. However, given the filters h_i, the norms $\|\psi_i\|$, $\|\phi\|$ can be conveniently calculated by defining the autocorrelation functions $s(t)$ and $w_i(t)$ and by

then evaluating them at $t = 0$. Let

$$s(t) := \phi(t) * \phi(-t) = \int \phi(\tau)\phi(\tau + t)\, d\tau,$$

$$w_i(t) := \psi_i(t) * \psi_i(-t) = \int \psi_i(\tau)\psi_i(\tau + t)\, d\tau, \qquad i = 1, 2.$$

Then $s(0) = \|\phi(t)\|^2$ and $w_i(0) = \|\psi_i(t)\|^2$. It can be shown that the autocorrelation functions $s(t)$ and $w_i(t)$ satisfy dilation and wavelet equations, as do $\phi(t)$ and $\psi_i(t)$,

$$s(t) = \sqrt{2} \sum_n r_0(n) s(t - n),$$

$$w_i(t) = \sqrt{2} \sum_n r_i(n) s(t - n), \qquad i = 1, 2,$$

where r_i are the discrete-time autocorrelation sequences of the filters h_i:

$$r_i(n) := \frac{1}{\sqrt{2}} h_i(n) * h_i(-n),$$

$$= \frac{1}{\sqrt{2}} \sum_k h_i(k) h_i(k + n), \qquad i = 0, 1, 2.$$

Therefore, samples of $s(t)$ and $w_i(t)$ can be computed using the same methods used to compute samples of $\phi(t)$ and $\psi(t)$, described in [5, 37] for example. In particular, $s(0)$ and $w_i(0)$ can be obtained.

As $\int \phi(t)\, dt = 1$, we also have $\int s(t)\, dt = 1$. (The integral of a convolution is the product of the integrals.) This normalization condition is needed so that the samples of $s(t)$, $w_i(t)$ can be obtained correctly.

2.5. Filter Banks

Just as Mallat's algorithm for computing a wavelet expansion of a signal from its fine-scale scaling coefficients $c(k)$ can be implemented by iterating a critically sampled two-channel filter bank, a wavelet frame of the type described above corresponds to the oversampled filter bank illustrated in Fig. 1. It also gives an overcomplete discrete-time signal expansion (a frame for $l_2(\mathbb{Z})$).

Wavelet frames, having the form described above, have twice as many wavelets than is necessary. Yet note that the corresponding filter bank illustrated in Fig. 1 is oversampled by $3/2$, not by 2. However, if the filter bank is iterated a single time on its lowpass branch (h_0), the total oversampling rate will be $7/4$. For a three-stage filter bank, illustrated in Fig. 2, the oversampling rate will be $15/8$. When this filter bank is iterated on its lowpass

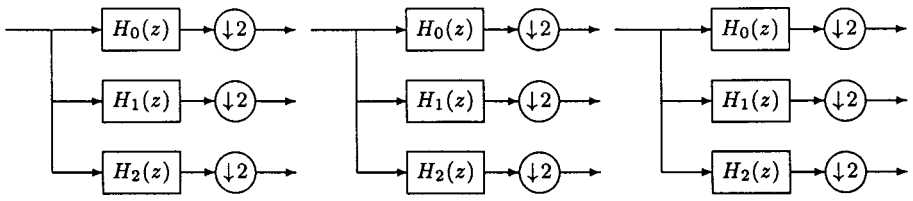

FIG. 2. An iterated oversampled filter bank.

branch indefinitely, the total oversampling rate increases toward 2, which is consistent with the redundancy of the frame for $L_2(\mathbb{R})$.

The "algorithme á trous" or undecimated DWT, is based on the iteration of an undecimated two-channel filter bank. Note that an l-stage filter bank of this type gives $l+1$ output samples for each input sample—it is redundant by a factor of $l+1$. Therefore, although this overcomplete expansion system is exactly shift invariant, it has an oversampling rate that increases without bound as the filter bank is iterated indefinitely, and although only a finite number of levels can be implemented in practice, the high degree of redundancy can make the undecimated DWT impractical for very large multidimensional data sets.

Even though both the filter bank illustrated in Fig. 2 and the iterated undecimated filter bank (on which the UDWT is based) are oversampled, they lead to overcomplete signal expansions having very different rates of redundancy. In the first case, the redundancy is bounded by 2, while in the second case, the redundancy grows with the number of scales over which the signal is analyzed.

2.6. Frame Conditions

For the oversampled filter bank of Fig. 1 we have by standard multirate identities the relation,

$$\begin{aligned} Y(z) = \frac{1}{2}[H_0(z)H_0(1/z) + H_1(z)H_1(1/z) + H_2(z)H_2(1/z)]X(z) \\ + \frac{1}{2}[H_0(-z)H_0(1/z) + H_1(-z)H_1(1/z) + H_2(-z)H_2(1/z)]X(-z). \end{aligned}$$

Therefore, for h_0, h_1, h_2 to generate a tight frame, it is necessary that they satisfy the perfect reconstruction equations

$$H_0(z)H_0(1/z) + H_1(z)H_1(1/z) + H_2(z)H_2(1/z) = 2 \tag{3}$$

and

$$H_0(-z)H_0(1/z) + H_1(-z)H_1(1/z) + H_2(-z)H_2(1/z) = 0. \tag{4}$$

For detailed descriptions of oversampled PR filter banks, see for example [4, 11, 22].

2.7. Discrete-Time Wavelet Tight Frame Expansions

The iterated oversampled filter bank provides an overcomplete discrete-time expansion (a frame for $l_2(\mathbb{Z})$). Following the exposition and notation of, for example, [38, Section 3.3.1], we denote the iterated filters that form the discrete-time frame by $h_i^{(j)}$. In a tight frame filter bank with J stages, the iterated filters are given by

$$H_0^{(J)}(z) = \prod_{k=0}^{J-1} H_0(z^{(2^k)})$$

$$H_i^{(j)}(z) = H_i(z^{2^{(j-1)}}) \prod_{k=0}^{j-2} H_0(z^{(2^k)}), \qquad i = 1, 2,\ j = 1, \ldots, J.$$

Then any sequence $x(n) \in l_2(\mathbb{Z})$ can be written as a linear combination of $h_0^{(J)}(n - 2^J k)$, $h_i^{(j)}(n - 2^j k)$, $i = 1, 2$, $j = 0, \ldots, J$, $k \in \mathbb{Z}$, where the weights are given by $\langle h_0^{(J)}(2^J k - n), x(n)\rangle$, $\langle h_i^{(j)}(2^j k - n), x(n)\rangle$.

An important difference between discrete-time orthonormal expansions and tight frame expansion of this type is the following: Not only are the norms of h_i unequal, the norms of the iterated filters $h_i^{(j)}$ for different values of j are also unequal. In the orthonormal case $\|h_i^{(j)}\| = 1$ for all j, but in the case of tight frames $\|h_i^{(j)}\| \neq \|h_i^{(j+1)}\|$. Quantization and threshold levels must be adjusted according to $\|h_i^{(j)}\|$. However, as j increases, their norms converge to the norms of the continuous-time functions $\phi(t)$, $\psi_i(t)$, as will be illustrated in the examples below.

3. NEW EXAMPLES

We seek to design FIR filters h_0, h_i, h_2 that generate tight frames of the form described in (1). The filters also generate discrete-time tight frames via the iteration of oversampled filter banks. We seek the shortest filters h_i having a prescribed number of zeros at $z = -1$ and $z = 1$ (specified by the values K_i) that satisfy the tight frame conditions (3), (4). In the examples, we ask that $K_1 = K_2$. If they are unequal, then one wavelet annihilates more polynomials than the other, or one wavelet is doing "more work" than the other.

Note that the conditions (3), (4) are nonlinear equations in the filter coefficients $h_i(n)$. For the design problems considered below, these nonlinear design equations will be handled using Gröbner bases, a powerful but computationally expensive tool from computational algebraic geometry [10]. In a loose sense, Gröbner bases extend the Gaussian elimination of variables to polynomial systems of equations. The Gröbner bases are too big to include in the paper, but they are available on the author's Webpage. For previous applications of Gröbner bases to the design of wavelets and filters, see for example [13, 24, 27, 32–34].

3.1. Example 1—(K_0, K_1, K_2) = (3,1,1)

For the first example, we ask that $K_0 = 3$, $K_1 = K_2 = 1$. It was found that the shortest filters h_0, h_1, h_2 satisfying (3), (4) are of length 4, 4, and 2, respectively. The filters are given by

$$H_0(z) = \frac{\sqrt{2}}{8}\left(1 + z^{-1}\right)^3$$

$$H_1(z) = \frac{\sqrt{2}}{8}\left(1 - z^{-1}\right)\left(1 + 4z^{-1} + z^{-2}\right)$$

$$H_2(z) = \frac{\sqrt{6}}{4}\left(1 - z^{-1}\right).$$

This system was found independently in [7] by a different approach. The filters and the wavelet functions are illustrated in Fig. 3. $\phi(t)$ is symmetric, $\psi_i(t)$ are anti-symmetric. Note that $\phi(t)$ is especially smooth given its support. On the other hand, it is important to note that the wavelets have only one zero moment: $\int \psi_i(t)\, dt = 0$, but $\int t\psi_i(t)\, dt \neq 0$. The analysis filter bank annihilates constant signals $x(n) = c$, but does not annihilate ramp signals $x(n) = c \cdot n$.

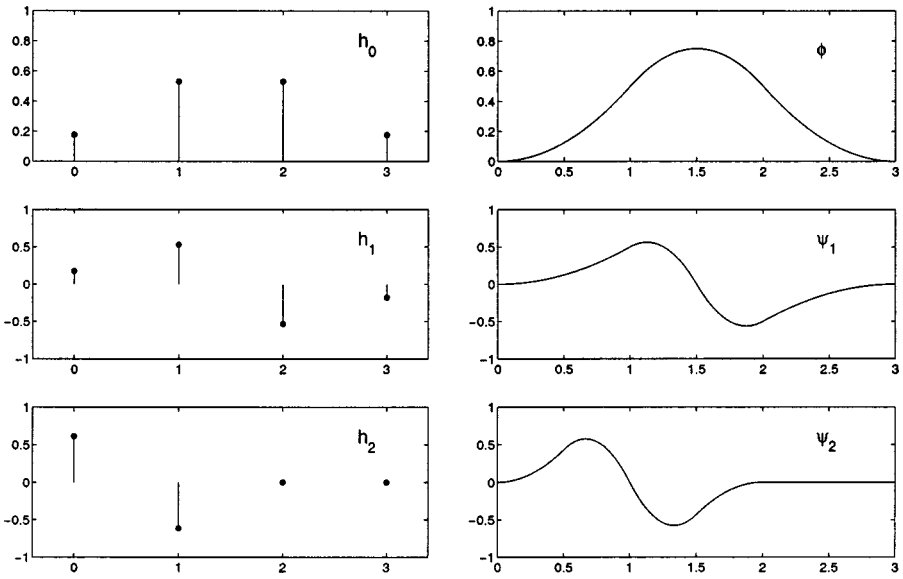

FIG. 3. The generators of a wavelet tight frame with parameters $K_0 = 3$, $K_1 = K_2 = 1$.

Due to the simple form of h_0, the scaling function $\phi(t)$ is a B spline, obtained by convolving a square pulse $p(t)$ with itself: $\phi(t) = p(t) * p(t) * p(t)$. Therefore, closed form expressions for ϕ, ψ_i can be obtained for this example. Note that the norms of ϕ, ψ_i are unequal

$$\|\phi(t)\| = \sqrt{0.55} \approx 0.7416$$
$$\|\psi_1(t)\| = \sqrt{0.30} \approx 0.5477$$
$$\|\psi_2(t)\| = \sqrt{0.25} \approx 0.5,$$

but note also that $\|\phi(t)\|^2 = \|\psi_1(t)\|^2 + \|\psi_2(t)\|^2$; i.e., the energy of the scaling function equals the total energy of the wavelets.

As mentioned above, the iterated filters $h_i^{(j)}$ have different norms at different scales j. The norms of these iterated filters, shown in Table 1, are needed, so that quantization and thresholding levels can be properly chosen in applications. The norms of the iterated filters converge to the norms of the scaling and wavelet functions, as evident in Table 1. $\|h_0^{(j)}\| \to \|\phi\|$, $\|h_i^{(j)}\| \to \|\psi_i\|$. Therefore, it is important to keep track of the norms only for the first few stages.

Note that the centers of symmetry of h_1 and h_2 are offset by a single sample. Accordingly, the centers of symmetry of ψ_1 and ψ_2 are offset by exactly one-half. $h_1(n)$ is centered halfway between $h_2(n)$ and $h_2(n-1)$. $\psi_1(t)$ is likewise centered between $\psi_2(t)$ and $\psi_2(t-1)$. In particular, $\phi_1(t) \approx \psi_2(t - \frac{1}{2})$. Having more wavelets than necessary gives a closer spacing between adjacent wavelets within the same scale. It is this property that makes this system less shift-sensitive than a nonredundant system.

Also, note that $K_0 + K_1 = 4$, the length of h_0. While K_i are more free than in the orthonormal case, there is still the constraint that the minimum length of the filter h_0 is $K_0 + \min\{K_1, K_2\}$.

TABLE 1
Norms of the Iterated Filters in Example 1

j	$\|h_0^{(j)}\|$	$\|h_1^{(j)}\|$	$\|h_2^{(j)}\|$
1	0.7906	0.7906	0.8660
2	0.7526	0.5962	0.5728
3	0.7443	0.5588	0.5163
4	0.7423	0.5504	0.5040
5	0.7418	0.5484	0.5010
6	0.7417	0.5479	0.5002
7	0.7416	0.5478	0.5001
8	0.7416	0.5477	0.5000
9	0.7416	0.5477	0.5000
	⋮	⋮	⋮

3.2. Example 2—(K_0, K_1, K_2) = (5,2,2)

For the second example, we ask that $K_0 = 5$, $K_1 = K_2 = 2$. It was found that the shortest filters h_0, h_1, h_2 satisfying (3), (4) are of length 7, 7, and 5, respectively.

This example does not appear to admit simple expressions for the coefficients $h_i(n)$, as the nonlinear design equations are much more complex. In particular, each of the transfer functions $H_i(z)$ has zeros away from $z = -1$ and $z = 1$, making the system of equations more complicated. However, by utilizing Gröbner basis methods [10] it is possible to solve the equations algebraically. (*Singular* [16] was used for the Gröbner basis calculations.) The original design equations have only rational coefficients, and we were able to obtain explicit expressions for $h_i(n)$ in terms of radicals. The expressions obtained for $h_i(n)$ are too long to include here, but are available from the author. However, the expressions for the autocorrelation sequences $r_i(n)$, from which h_i can be obtained via spectral factorization, are short enough to give in Table 2. The coefficients of the autocorrelation sequences are not rational, but require a root A of the fourth degree polynomial:

$$\begin{aligned} p(A) = {} & 193790354134538781720576A^4 - 391574453567833132498944A^3 \\ & + 296647402984779246206976A^2 - 99861551659146071783424A \\ & + 12603835548400234105441. \end{aligned} \tag{5}$$

As in the orthonormal case, there are multiple solutions to this problem. However, in contrast to the orthonormal case, (i) the distinct solutions do not all share the same autocorrelation, and (ii) not all of the spectral factors of r_i (for a particular root A) are solutions.

In this example, there are four distinct solutions, not counting their time reversals ($h_i(-n)$) and negations ($-h_i(n)$). For none of them are the filters h_i symmetric or anti-symmetric. One solution, obtained with the root $A \approx 0.5068$, is shown in Fig. 4. The numerical values for this solution are given in Table 2. For this solution h_0 and h_2 are the minimum- and maximum-phase spectral factors of r_0, r_2, respectively.

Because this solution is not symmetric, we cannot say exactly that $\psi_1(t)$ lies halfway between $\psi_2(t)$ and $\psi_2(t-1)$, but it is roughly correct. In addition to visual inspection,

TABLE 2
Coefficients r_i for Example 2, where A Must Be a Root of the Polynomial $p(A)$ in (5)

$\pm n$	$\sqrt{2}r_0(n)$	$\sqrt{2}r_1(n)$	$\sqrt{2}r_2(n)$
0	357/512	A	$-A+667/512$
1	135/256	$-294A/95+2219/1520$	$294A/95-48329/24320$
2	405/2048	$282A/95-325571/194560$	$-282A/95+35887/24320$
3	$-5/512$	$2A/5-589/2560$	$-2A/5+307/1280$
4	$-45/1024$	$-147A/190+10301/24320$	$147A/190-36929/97280$
5	$-9/512$	9/512	0
6	$-5/2048$	5/2048	0

n	$h_0(n)$	$h_1(n)$	$h_2(n)$
0	0.07622367464861	-0.02054794025163	-0.02716023598942
1	0.34908887241859	-0.09410537245854	-0.12438833734897
2	0.60208924236383	-0.12289782090121	-0.13016597007712
3	0.44194173824159	0.06135335608384	0.74213789615884
4	0.06082336499856	0.60633280881675	-0.46042335274333
5	-0.08392382947363	-0.31131989847772	0
6	-0.03202950082445	-0.11881513281150	0

Note. Coefficients h_i corresponding to $A \approx 0.5068$.

one way to illustrate that $h_1(n)$ is approximately offset from $h_2(n)$ by one sample is to plot the group delay function $G_i(\omega)$ of h_1 and h_2, which reveals that $G_1(\omega) \approx G_2(\omega) + 1$. As in the first example, this system is less sensitive to shifts than a similar nonredundant basis.

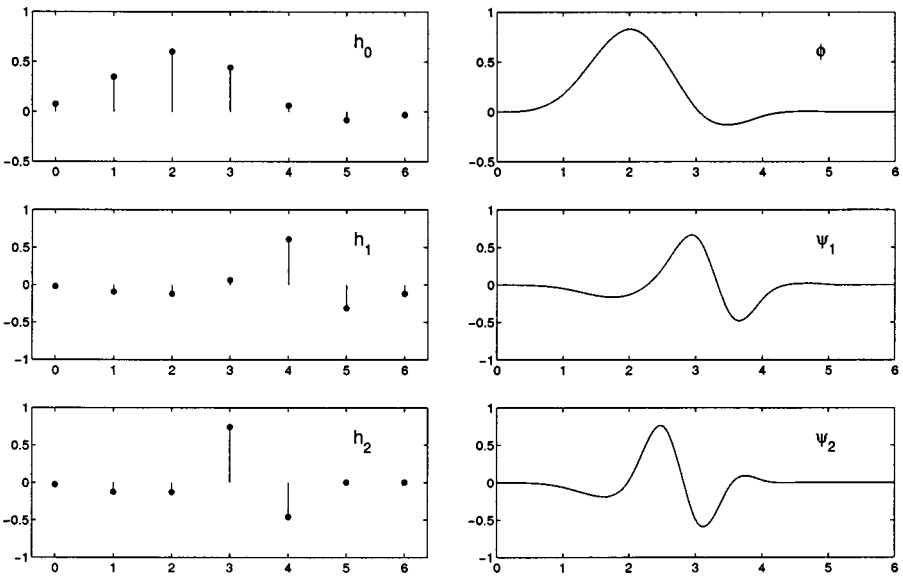

FIG. 4. The generators of a wavelet tight frame with parameters $K_0 = 5$, $K_1 = K_2 = 2$. The coefficients h_i are given in Table 2.

TABLE 3
Coefficients h_i for Example 3

n	$h_0(n)$	$h_1(n)$	$h_2(n)$
0	0.03199264772465	0.00293054941766	0.00431490224412
1	0.19632717543243	0.01798370971314	0.02647897658069
2	0.48517334610839	0.03894655182791	0.04889472840408
3	0.58643491952102	0.01999291879950	−0.02241516250771
4	0.29321745976051	−0.07153466971605	−0.20001902951146
5	−0.06119804718367	−0.19870485906190	−0.24219681629703
6	−0.12239609436734	−0.14562293679897	0.74055955394590
7	−0.02113452095472	0.61762964054644	−0.35561715285859
8	0.01911942196034	−0.20872568392457	0
9	0.00667725437149	−0.07289522080316	0

For this example, the scaling function ϕ is not a spline as it was for the first example. However, the norms of the ϕ, ψ_i can be found as described in Section 2.4 above. Again, their norms are unequal,

$$\|\phi(t)\| = 0.8221390, \qquad \|\psi_1(t)\| = 0.5589626, \qquad \|\psi_2(t)\| = 0.6028876,$$

and again $\|\phi(t)\|^2 = \|\psi_1(t)\|^2 + \|\psi_2(t)\|^2$. The norms of the iterated filters $h_i^{(j)}$ converge to the norms of ϕ, ψ_i to within four decimal places by $j = 5$.

3.3. Example 3—(K_0, K_1, K_2) = (7,3,3)

For the third example, we ask that $K_0 = 7$, $K_1 = K_2 = 3$, for which the shortest filters h_0, h_1, h_2 forming a tight frame are of length 10, 10, and 8, respectively.

Again, we used Gröbner bases to solve the nonlinear design equations and we obtained explicit solutions for h_i in terms of radicals. There are exactly eight distinct solutions, not counting their time reversals ($h_i(-n)$) and negations ($-h_i(n)$). One of those eight solutions, the coefficients of which are given in Table 3, is shown in Fig. 5. The other seven solutions are tabulated on the author's Webpage. The norms of the scaling and wavelet functions are

$$\|\phi(t)\| = 0.8462926, \qquad \|\psi_1(t)\| = 0.5567725, \qquad \|\psi_2(t)\| = 0.6373504,$$

which satisfy $\|\phi(t)\|^2 = \|\psi_1(t)\|^2 + \|\psi_2(t)\|^2$. The norms of the iterated filters $h_i^{(j)}$ converge to the norms of ϕ, ψ_i to within four decimal places by $j = 4$.

4. MAXIMALLY FLAT FILTERS

Due to the constraint (2), if $H_1(z)$ and $H_2(z)$ have at least M zeros at $z = 1$, then the first $M - 1$ derivatives of $|H_0(e^{j\omega})|$ at $\omega = 0$ must be zero. Therefore, the minimal length lowpass filter h_0 can be obtained by spectral factorization of a maximally flat symmetric FIR filter, a family of filters originally described by Herrmann [17]. Specifically, letting

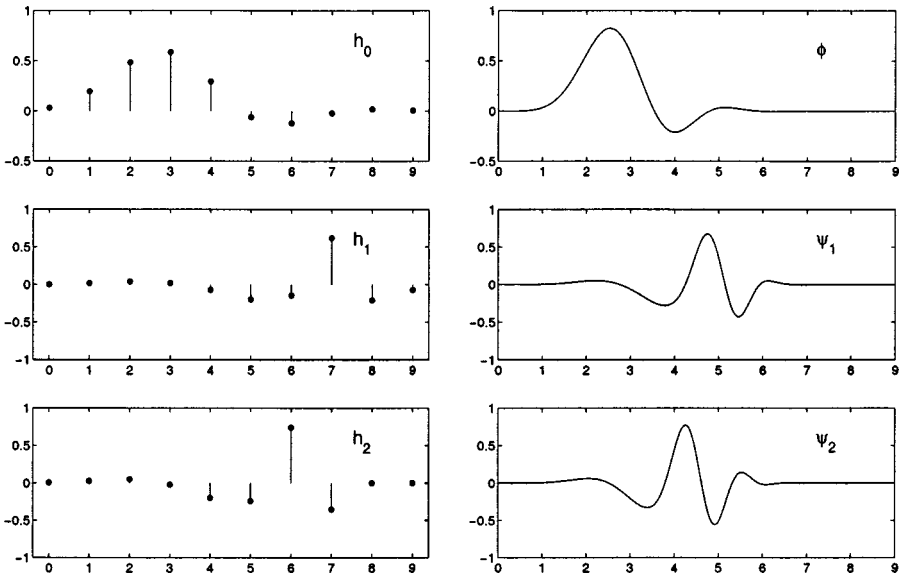

FIG. 5. The generators of a wavelet tight frame with parameters $K_0 = 7$, $K_1 = K_2 = 3$. The coefficients h_i are given in Table 3.

$M = \min(K_1, K_2)$, one has

$$|H_0(e^{j\omega})|^2 = 2(1-y)^{K_0} \sum_{k=0}^{M-1} \binom{K_0 - 1 + k}{k} y^k, \tag{6}$$

where $y = \frac{1}{2}(1 - \cos\omega)$. When $M = K_0$, this formula specializes to the Daubechies polynomial, that is, the polynomial that is used in Daubechies' construction of short orthonormal wavelets [12]. The Daubechies polynomial is the halfband instance of the maximally flat filter. The filter here is of the same maximally flat family, but rather than being halfband, it has instead a higher degree of flatness at $\omega = \pi$ than at $\omega = 0$. That makes the passband more narrow than the stopband and increases the smoothness of $\phi(t)$.

While formula (6) yields directly a formula for $r_0(n)$ from which $h_0(n)$ can be obtained through spectral factorization, it does not yield the filters $h_1(n)$, $h_2(n)$.

5. NEAR SHIFT-INVARIANCE

For the type of tight frame presented above, the (idealized) time-frequency localization of the wavelets are indicated in Fig. 6. Each scale is represented by twice as many wavelets as in the critically sampled case. In this way, the tight frame DWT approximates the continuous wavelet transform more closely than does the critically sampled DWT, and consequently it is more robust to shifts than the critically sampled DWT.

Kingsbury demonstrated the near shift-invariance of the dual-tree DWT in [19, 21] by reconstructing a shifted discrete-time step function $u(n - n_0)$ from only its wavelet coefficients at a single scale j. Varying the shift n_0 in increments of 1, the results reveal the shift-varying properties of the system. Following the same procedure, for $j = 1, 2, 3, 4$,

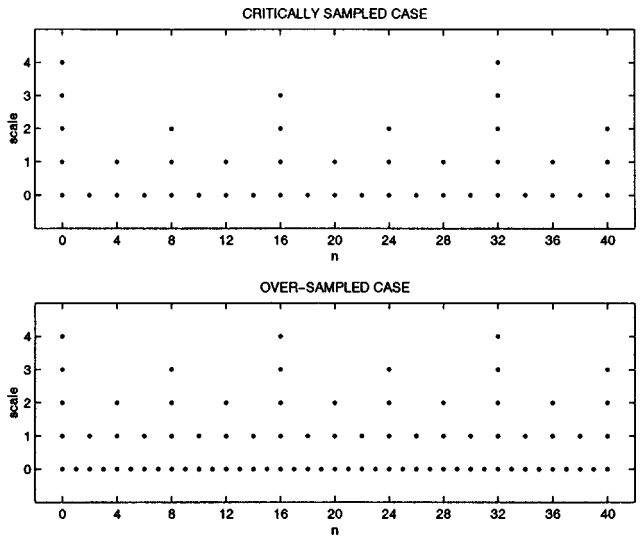

FIG. 6. Idealized time-frequency localization diagrams. The tight frame gives a denser sampling of the time-frequency plane.

the left-hand side of Fig. 7 illustrates the near shift invariance of the oversampled filter bank of Example 3 tabulated in Table 3. For comparison, the right-hand side uses Daubechies' orthonormal basis D_5 (length $h_0 = 10$) [12]. The top panels show the reconstruction

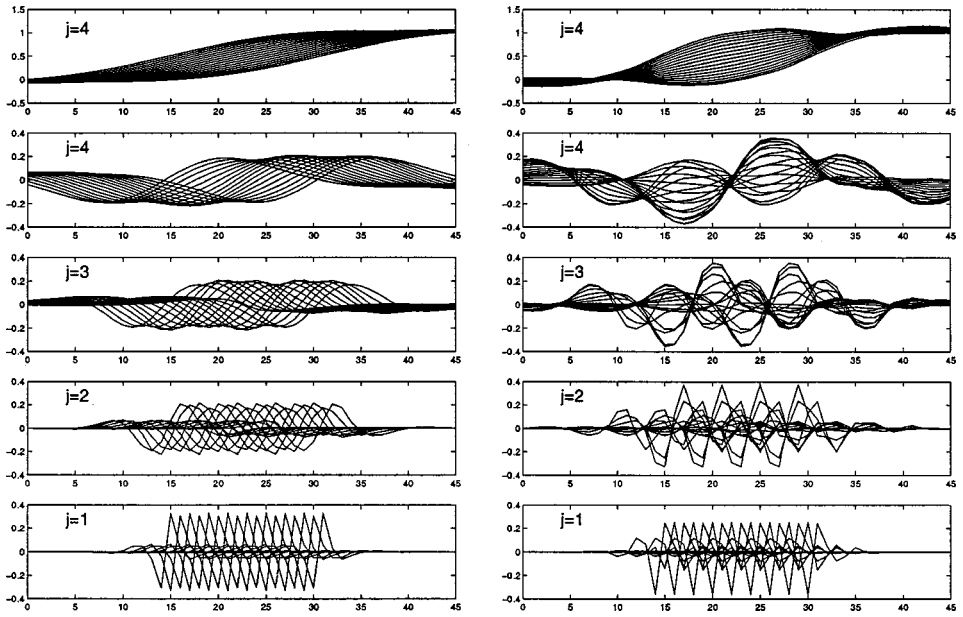

FIG. 7. Reconstruction of $u(n - n_0)$ from coefficients at level j only. (Left) The decomposition uses the wavelet tight frame illustrated in Fig. 5. (Right) The decomposition uses Daubechies' orthonormal basis D_5 ($h_0 = 10$). The tight frame is less shift-sensitive than the orthonormal basis.

from only the scaling coefficients at level $j = 4$. Although the overcomplete expansion of Example 3 is not as shift-insensitive as the dual-tree DWT presented in [21], it is much less shift-sensitive than the orthonormal basis, as illustrated in Fig. 7.

It should be noted that other orthonormal bases may be less shift-sensitive than Daubechies' bases, for example, those designed in [2]; however, the shift-sensitivity properties of orthonormal wavelet bases are naturally limited in comparison with tight wavelet frames due to their nonredundancy.

6. 2D EXTENSION

Separable 2D wavelet frames can be obtained by alternating between rows and columns, as is usually done for 2D separable DWTs. The corresponding filter bank, illustrated in Fig. 8, is iterated on the lowpass branch (the first branch). While the 1D frames based on the oversampled filter banks described above (iterated indefinitely) are redundant by a factor of 2, the corresponding 2D version is redundant by a factor of $8/3$, not by 2 or 4 as one might initially expect.

In the oversampled filter bank for the 2D case, the 1D oversampled filter bank is iterated on the rows and then on the columns. This gives rise to nine 2D branches. One of the branches is a 2D lowpass scaling filter, while the other eight make up the eight 2D wavelet filters. Note that for a critically sampled 2D filter bank, there are three wavelet filters; hence the rate of oversampling, when the structure is iterated indefinitely, is $8/3$. In general, the redundancy rate is $(3^d - 1)/(2^d - 1)$ for the extension to d-dimensional signals. Note that as d increases, this ratio approaches $(3/2)^d$, the oversampling rate of the filter bank building block. This is higher than the redundancy of a 2D Laplacian pyramid [6], but lower than the 2D dual tree. The 2D extension of the dual-tree DWT has a redundancy rate of 4. In general, the d-dimensional dual-tree has a redundancy of 2^d [21]. It should be noted that the steerable pyramid [14] is another example of a system that gives an overcomplete signal decomposition. They are especially designed to yield orientation information of image components.

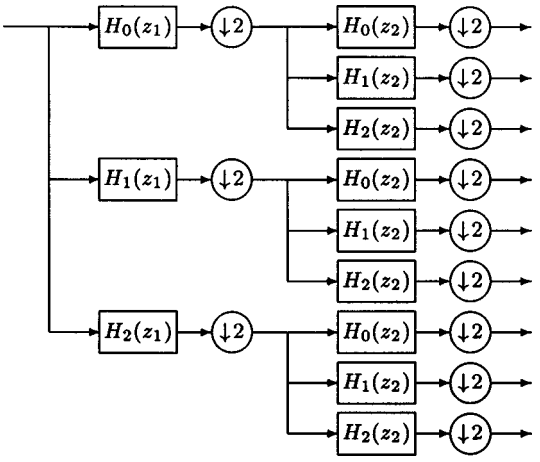

FIG. 8. An oversampled filter bank for 2D signals.

6.1. Rectangular Artifacts

Following Kingsbury's illustration, the improved behavior of the redundant 2D wavelet frame transform in 2D can be indicated by projecting the image of a disk onto the wavelet spaces and the scaling space. In Fig. 9 the image of a disk is reconstructed from different

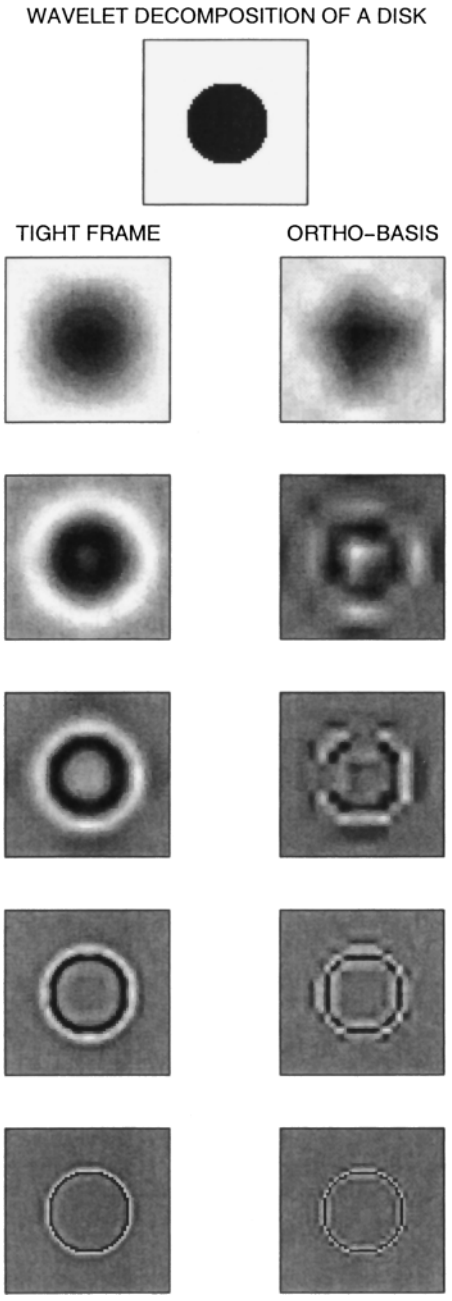

FIG. 9. Reconstruction of the image of a disk from coefficients at level j only. (Left) The decomposition uses the tight wavelet frame illustrated in Fig. 4. (Right) The decomposition uses the most symmetric form of Daubechies' orthonormal wavelet basis D_4 (length $h_0 = 8$).

levels of a 4-scale decomposition. The image is 64 by 64 pixels. On the left side of the figure, the decomposition is performed using the wavelet tight frame illustrated in Fig. 4. On the right side of the figure, the decomposition is performed using the most symmetric case of Daubechies' orthonormal wavelet D_4 filters (length $h_0 = 8$). In each column, the top-most panel is obtained by reconstructing the image from the coarse scaling coefficients, while the following panels are obtained by reconstructing from the wavelet coefficients in scales $j = 1, 2, 3, 4$. It is clear that the decomposition using the tight frame suffers from fewer of the rectangular artifacts than the decomposition using the orthonormal basis. Similar figures are obtained if the other tight frame examples given above are used, or if other orthonormal bases are used.

7. CONCLUSION

Kingsbury showed that the shift sensitivity of the DWT can be dramatically improved by using a dual tree, an overcomplete expansion that is redundant by a factor of 2 only. So motivated, this paper considered the design of wavelet tight frames based on iterated oversampled filter banks as in [7, 30, 31]. In particular, we consider the design of wavelet tight frames that are analogous to Daubechies orthonormal wavelets bases. As the number of zeros $H_0(z)$ has at $\omega = \pi$ need not equal the number of zeros $H_1(z)$ and $H_2(z)$ have at $\omega = 0$, there is more design freedom than in the orthonormal case. Although the resulting design equations are nonlinear, Gröbner bases can be used to obtain the solutions. By asking that $K_0 > K_1, K_2$, wavelets are obtained that are very smooth in comparison with orthonormal wavelet bases. Like the dual-tree DWT of Kingsbury, the overcomplete DWT described above is less shift-sensitive than an orthonormal wavelet basis (and in the 2D case has fewer rectangular artifacts).

The complete solutions to the examples examined in this paper and other examples are available on the author's Webpage: `taco.poly.edu/selesi`. Also available are the *Singular* programs for obtaining the Gröbner bases from which the solutions are obtained.

ACKNOWLEDGMENTS

The author thanks Nick Kingsbury for helpful conversations about the dual-tree DWT and anonymous reviewers for valuable comments. The author also gratefully acknowledges support by the NSF under CAREER Grant CCR-987452.

REFERENCES

1. J. J. Benedetto and S. Li, The theory of multiresolution an analysis frames and applications to filter banks, *Appl. Comput. Harmon. Anal.* **5** (1998), 389–427.
2. S. A. Benno and J. M. F. Moura, Scaling functions robust to translations, *IEEE Trans. Signal Process.* **46** (1998), 3269–3281.
3. K. Berkner and R. O. Wells, Jr., A correlation-dependent model for denoising via nonorthogonal wavelet transforms, Technical Report CML TR98-07, Computational Mathematics Laboratory, Rice University, 1998.
4. H. Bölcskei, F. Hlawatsch, and H. G. Feichtinger, Frame-theoretic analysis of oversampled filter banks, *IEEE Trans. Signal Process.* **46** (1998), 3256–3268.
5. C. S. Burrus, R. A. Gopinath, and H. Guo, "Introduction to Wavelets and Wavelet Transforms," Prentice Hall, Englewood Cliffs, NJ, 1997.

6. P. J. Burt and E. H. Adelson, The Laplacian pyramid as a compact image code, *IEEE Trans. Comm.* **31** (1983), 532–540.
7. C. Chui and W. He, Compactly supported tight frames associated with refinable functions, *Appl. Comput. Harmon. Anal.* **8** (2000), 293–319.
8. C. K. Chui, X. Shi, and J. Stöckler, Affine frames, quasi-affine frames, and their duals, *Adv. Comp. Math.* **8** (1998), 1–17.
9. R. R. Coifman and D. L. Donoho, Translation-invariant de-noising, in "Wavelets and Statistics" (A. Antoniadis, Ed.), Springer-Verlag Lecture Notes, Springer-Verlag, Berlin, 1995.
10. D. Cox, J. Little, and D. O'Shea, "Ideals, Varieties, and Algorithms: An Introduction to Computational Algebraic Geometry and Commutative Algebra," Springer-Verlag, Berlin, 1991.
11. Z. Cvetkovič and M. Vetterli, Oversampled filter banks, *IEEE Trans. Signal Process.* **46** (1998), 1245–1255.
12. I. Daubechies, "Ten Lectures on Wavelets," SIAM, Philadelphia, 1992.
13. J.-C. Faugère, F. M. de Saint-Martin, and F. Rouillier, Design of regular nonseparable bidimensional wavelets using Gröbner basis techniques, *IEEE Trans. Signal Process.* **46** (1998), 845–856.
14. W. T. Freeman and E. H. Adelson, The design and use of steerable filters, *IEEE Trans. Pattern Anal. Mach. Intell.* **13** (1991), 891–906.
15. V. K. Goyal, M. Vetterli, and N. T. Thao, Quantized overcomplete expansions in $\mathbb{R}^N$: Analysis, synthesis and algorithms, *IEEE Trans. Inform. Theory* **44** (1998), 16–31.
16. G.-M. Greuel, G. Pfister, and H. Schönemann, Singular reference manual, in "Reports on Computer Algebra," number 12, Centre for Computer Algebra, University of Kaiserslautern, May 1997. Available at http://www.singular.uni-kl.de/.
17. O. Hermann, On the approximation problem in nonrecursive digital filter design, *IEEE Trans. Circuit Theory* **18** (1971), 411–413. Reprinted in Ref. [28].
18. M. Holschneider, R. Kronland-Martinet, J. Morlet, and Ph. Tchamitchian, A real-time algorithm for signal analysis with the help of the wavelet transform, in "Wavelets, Time-Frequency Methods and Phase Space" (J. M. Combes, A. Grassman, and Ph. Tchamitchian, Eds.), pp. 286–297, Springer-Verlag, Berlin, 1989.
19. N. G. Kingsbury, The dual-tree complex wavelet transform: A new technique for shift invariance and directional filters, in "Proceedings of the Eighth IEEE DSP Workshop, Utah, August 9–12, 1998."
20. N. G. Kingsbury, Image processing with complex wavelets, *Phil. Trans. R. Soc. London A* Sept. (1999).
21. N. G. Kingsbury, Shift invariant properties of the dual-tree complex wavelet transform, in "Proc IEEE Int. Conf. Acoust., Speech, Signal Processing (ICASSP), Phoenix, March 16–19, 1999."
22. J. Kliewer and A. Mertins, Oversampled cosine-modulated filter banks with arbitrary system delay, *IEEE Trans. Signal Process.* **46** (1998), 941–955.
23. M. Lang, H. Guo, J. E. Odegard, C. S. Burrus, and R. O. Wells, Jr., Noise reduction using an undecimated discrete wavelet transform, *IEEE Signal Process. Lett.* **3** (1996), 10–12.
24. J. Lebrun and M. Vetterli, High order balanced multiwavelets: Theory, factorization and design, preprint, 1998.
25. N. J. Munch, Noise reduction in tight Weyl–Heisenberg frames, *IEEE Trans. Inform. Theory* **38** (1992), 608–616.
26. G. P. Nason and B. W. Silverman, Stationary wavelet transform and some statistical applications, in "Wavelets and Statistics" (A. Antoniadis, Ed.), pp. 281–299, Springer-Verlag Lecture Notes, Springer-Verlag, Berlin, 1995.
27. H. Park, T. Kalker, and M. Vetterli, Groebner bases and multidimensional FIR multirate systems, *J. Multidimen. Syst. Signal Process.* **8** (1997), 11–30.
28. L. R. Rabiner and C. M. Rader (Eds.), "Digital Signal Processing," IEEE Press, New York, 1972.
29. O. Rioul and P. Duhamel, Fast algorithms for discrete and continuous wavelet transforms, *IEEE Trans. Inform. Theory* **38** (1992), 569–586.
30. A. Ron and Z. Shen, Affine systems in $L_2(\mathbb{R}^d)$: The analysis of the analysis operator, *J. Funct. Anal.* **148** (1997), 408–447.
31. A. Ron and Z. Shen, Construction of compactly supported affine frames in $L_2(\mathbb{R}^d)$, in "Advances in Wavelets" (K. S. Lau, Ed.), Springer-Verlag, Berlin, 1998.

32. I. W. Selesnick, Interpolating multiwavelet bases and the sampling theorem, *IEEE Trans. Signal Process.* **47** (1999), 1615–1621.
33. I. W. Selesnick, Balanced multiwavelet based on symmetric FIR filters, *IEEE Trans. Signal Process.* **48** (2000), 184–191.
34. I. W. Selesnick and C. S. Burrus, Maximally flat low-pass FIR filters with reduced delay, *IEEE Trans. Circuits Syst. II* **45** (1998), 53–68.
35. I. W. Selesnick and L. Sendur, Iterated oversampled filter banks and wavelet frames, in "Wavelet Applications in Signal and Image Processing VIII, San Diego, 2000," Proceedings of SPIE, Vol. 4119.
36. M. J. Shensa, The discrete wavelet transform: Wedding the à trous and Mallat algorithms, *IEEE Trans. Signal Process.* **40** (1992), 2464–2482.
37. G. Strang and T. Nguyen, "Wavelets and Filter Banks," Wellesley-Cambridge Press, 1996.
38. M. Vetterli and J. Kovačević, "Wavelets and Subband Coding," Prentice-Hall, Englewood Cliffs, NJ, 1995.
39. Z. Xiong, M. T. Orchard, and Y.-Q. Zhang, A deblocking algorithm for JPEG compressed images using overcomplete wavelet representations, *IEEE Trans. Circuits Syst. Video Technol.* **7** (1997), 433–437.